Knockdown of *CYP6SZ3* and *CYP6AEL1* genes increases the susceptibility of *Lasioderma serricorne* to ethyl formate and benzothiazole

Xiaokun Li[†], Lixin Ma[†], Wenjia Yang and Kangkang Xu*

Key Laboratory of Surveillance and Management of Invasive Alien Species in Guizhou Education Department, Guiyang University, Guiyang, China

Insect cytochrome P450 monooxygenases (CYPs) play crucial roles in the metabolic detoxification of insecticides. Ethyl formate and benzothiazole have recently regained popularity as fumigants due to rising resistance to phosphine in the stored-product pests. However, the mechanisms underlying tolerance to these two fumigants in *Lasioderma serricorne*, a major global insect pest of stored products, remain poorly understood. In this study, two *CYP* genes, named *CYP6SZ3* and *CYP6AEL1*, were identified from *L. serricorne*, belonging to the CYP6 family and containing five conserved domains characteristic of CYP proteins. Spatiotemporal expression analysis revealed that both genes were predominantly expressed in the larval stage and showed the highest expression in the foregut. Upon exposure to ethyl formate and benzothiazole, both genes were upregulated, with significantly increased transcription levels following treatment. RNA interference-mediated silencing of *CYP6SZ3* and *CYP6AEL1* led to increased susceptibility and significantly higher mortality of *L. serricorne* when exposed to these fumigants. Homology modeling and molecular docking analyses showed stable binding of these fumigants to CYP6SZ3 and CYP6AEL1 proteins, with binding free energies from −26.88 to −94.68 kcal mol^{-1}. These findings suggest that the induction of *CYP6SZ3* and *CYP6AEL1* is likely involved in the detoxification of ethyl formate and benzothiazole in *L. serricorne*.

KEYWORDS

Lasioderma serricorne, cytochrome P450, gene expression, detoxification, molecular docking

1 Introduction

Insect cytochrome P450 monooxygenases (CYPs or P450s), encoded by a highly conserved superfamily of genes, are involved in the oxidative metabolism of both endogenous compounds (like fatty acids and hormones) and exogenous substrates (including chemical insecticides and plant allelochemicals) (Katsavou et al., 2022; Li et al., 2007; Schuler, 2011). Insect P450 enzymes typically consist of approximately 500 amino acids and possess a characteristic heme-binding domain with the FxxGxRxCxG recognition motif (Feyereisen and Gilbert, 2012). Although the number of CYP genes varies significantly across insect species, they are classified into six primary clans based on phylogenetic relationships: CYP2, CYP3, CYP4, mitochondrial CYP, and the CYP20 and CYP16 clans

(Dermauw et al., 2020). Substantial evidence highlights the roles of the CYP3 clan, particularly members of the CYP6 and CYP9 families, in xenobiotic metabolism and direct detoxification processes (Lu et al., 2021). Numerous CYPs involved in insecticide detoxification, predominantly from the CYP6 and CYP9 families, have been identified and functionally characterized. For example, RNA interference (RNAi)-mediated silencing of genes such as *CYP6DW4*, *CYP6DW5*, *CYP6DW6*, and *CYP6DZ8* greatly increased mortality of *Bemisia tabaci* to imidacloprid (Qin et al., 2023). Reducing the expression of *CYP9A9* significantly increased the susceptibility of *Spodoptera exigua* to lufenuron and methoxyfenozide (Zhang L. J. et al., 2023). Similarly, knockdown of *CYP6BQ7* in *Tribolium castaneum* reduced tolerance to essential oil of *Artemisia vulgaris*, linking this gene to plant toxicant detoxification (Zhang et al., 2021). In *Helicoverpa armigera*, knocking out the *CYP6AE* cluster by genome editing dramatically decreased survival rate of the insects when exposed to different insecticides and phytochemical toxins (Wang et al., 2018). Heterologous expression studies confirmed the enzymatic activities of various CYP6 and CYP9 proteins, such as *Helicoverpa armigera* CYP9A12 and CYP9A14, which can metabolize pyrethroid (Yang et al., 2008), *Laodelphax striatellus* CYP6AY3v2, which can metabolize imidacloprid and indoxacarb (Wang et al., 2017), *Chilo suppressalis* CYP6CV5, which metabolizes imidacloprid and chlorantraniliprole (Xu et al., 2024), and *Meligethes aeneus* CYP6BQ23, which metabolizes deltamethrin (Zimmer et al., 2014), *Cydia pomonella* CYP9A120 and *CYP9A121*, which metabolize lambda-cyhalothrin (Li et al., 2023). Functional expression of *Ceratitis capitata* CYP6A51 in transgenic *Drosophila melanogaster* demonstrated a significant decrease in pyrethroid tolerance, supported by *in vitro* metabolism assays (Tsakireli et al., 2019). These studies underscore the crucial role of *CYP6* and *CYP9* genes in insecticide detoxification.

Chemical fumigation remains a common and effective strategy for controlling stored insect pests, relying on high concentrations of gaseous agents to target pests (Austel et al., 2017). Widely used fumigants include phosphine (Nayak et al., 2020), sulfuryl fluoride, methyl bromide, carbonyl sulfide (Aribou and Ng, 2022), and allyl isothiocyanate (Zhang et al., 2017). However, the extensive use of these limited options has led to the development of fumigant resistance in insects, environmental pollution (Boyer et al., 2012), and regulatory restrictions on some fumigants, creating an urgent need for alternative approaches. Ethyl formate, a naturally occurring compound found in the atmosphere, soil, water, vegetation, and various foods (e.g., beer, wine, grapes, wheat, barley, raisin, rice, and cheese) (Zaitoon et al., 2021; Ren and Mahon, 2006), degrades into ethanol and formic acid upon air exposure (Haritos and Dojchinov, 2003). Ethyl formate is increasingly being evaluated as a fumigant against stored pests such *Scirtothrips dorsalis* (Kim et al., 2023), *Macchiademus diplopterus* (Smit et al., 2020), *Drosophila suzukii* (Zaitoon et al., 2021), and *Sitophilus oryzae* (Damcevski et al., 2010), with minimal toxicity to plants, crops, and food. Benzothiazole compounds possess diverse biological activities, including antimicrobial, anticancer, antifungal, anthelmintic, antileishmanial, and anticonvulsant properties (Mithlesh et al., 2010). Benzothiazole demonstrates potent ovicidal, larvicidal, pupicidal, and adulticidal effects against *T. castaneum* and disrupts normal feeding and digestion in *Bradysia odoriphaga* (Cui et al.,

2020a; Cui et al., 2020b; Zhao et al., 2016a). Sublethal concentrations of benzothiazole prolonged the developmental periods of eggs, larvae, pupae of *B. odoriphaga*, and decreased the survival rate and female fecundity (Zhao et al., 2016b).

The cigarette beetle, *Lasioderma serricorne* (Fabricius) (Coleoptera: Anobiidae), was first discovered in dried resin within the tomb of Tutankhamun (Maille et al., 2023). The larvae primarily feed on stored tobacco, grains, and other products, causing substantial economic losses (Baliota et al., 2023). Currently, the management of *L. serricorne* relies heavily on phosphine fumigation, which is becoming less effective due to the emergence of a resistant population (Edde, 2019; Sağlam et al., 2015). Ethyl formate fumigation has demonstrated high toxicity against *L. serricorne* eggs, pupae, and adults, suggesting a promising alternative for pest control (Kim et al., 2020). However, the detoxification mechanisms of *L. serricorne* for ethyl formate and benzothiazole remain poorly understood. Insights into P450-mediated detoxification pathways could aid in developing more effective pest management strategies. This study aimed to: (1) characterize the full-length open reading frames (ORFs) of two *CYP6* genes in *L. serricorne*; (2) examine the temporal and spatial expression profiles of *CYP6SZ3* and *CYP6AEL1*; (3) assess the transcriptional response of these genes to ethyl formate and benzothiazole exposure; (4) evaluate the roles of *CYP6SZ3* and *CYP6AEL1* in the detoxification of these fumigants; and (5) perform homology modeling and molecular docking analyses of CYP6SZ3 and CYP6AEL1 interactions with the fumigants.

2 Materials and methods

2.1 Insect rearing and chemicals

A population of *L. serricorne* was originally collected from Guiyang City, Guizhou Province, China (Yang et al., 2019). Larvae were reared in dried roots of *Angelica sinensis* at 28°C ± 1°C, with 40% ± 10% relative humidity, and kept in continuous darkness in a laboratory without insecticide exposure. Ethyl formate (≥98% purity) was obtained from Shanghai Aladdin Biochemical Technology Co., Ltd., Shanghai, China, while benzothiazole (>96% purity) was supplied by the TCI (Shanghai) Development Co., Ltd., Shanghai, China.

2.2 Toxicity bioassay

Toxicity tests were conducted using a sealed bottle method as described previously (Yan et al., 2020). Ethyl formate or benzothiazole was applied to a 1×1 cm filter paper strip attached near the cap of a wide-mouthed bottle. Fourth-instar larvae were then placed in the sealed bottles and exposed to the fumigants. A control group of larvae was kept without fumigant exposure. Mortality was recorded after 24 h, with immobile individuals considered dead. Each bioassay involved five fumigant concentrations and a control group, with three to eight replicates for each treatment. Thirty larvae were randomly selected for each replicate. The sublethal concentration (LC_{30}) values, median lethal concentration (LC_{50}) values, and 95% confidence intervals were determined using standard probit analysis in SPSS 20.0 software (SPSS Inc., Chicago, IL, United States).

TABLE 1 Toxicity of two fumigants against *L. serricorne*.

Fumigants	Slope ± SE	LC$_{30}$ (95% CL) (μL L^{-1})	LC$_{50}$ (95% CL) (μL L^{-1})	X^2	P	df
Ethyl formate	10.850 ± 1.172	19.344 (18.522, 19.976)	21.621 (21.038, 22.202)	4.752	0.98025	13
Benzosulfonazole	2.00 0 ± 0.086	396.751 (322.406, 456.231)	725.616 (652.747, 797.332)	98.238	0.00001	36

CL, confidence limits.

2.3 Gene cloning and bioinformatic analysis

Two *CYP6* cDNA sequences were identified from the *L. serricorne* transcriptome (SRR13065789) and confirmed by reverse-transcription polymerase chain reaction (RT-PCR) using gene-specific primers (Supplementary Table S1). The nomenclatures of two *CYP6* genes (*CYP6SZ3* and *CYP6AEL1*) were provided by Dr. David R. Nelson from the Cytochrome P450 Nomenclature Committee. Molecular weight and isoelectric points (pI) were analyzed using ExPASy (https://web.expasy.org/protparam/). Multiple sequence alignment was conducted with CLC Sequence Viewer 8 (Qiagen, Aarhus A/S, www.qiagenbioinformatics.com), and conserved motifs were predicted using GENEDOC. The phylogenetic analysis was performed using the protein sequences from the CYP3 clan of Coleoptera insects obtained from the National Center for Biotechnology Information. A phylogenetic tree was constructed by MEGA 7.0 software using the neighbor-joining method with 1,000 bootstrap replicates (Kumar et al., 2016).

2.4 Fumigant treatment and sample collection

The fourth-instar larvae were treated with the LC$_{30}$ and LC$_{50}$ concentrations of ethyl formate and benzothiazole using the sealed method as described above. The surviving larvae were collected at 24 h after fumigants treatment. For each treatment, thirty individuals were used, with three replicates per treatment. Different developmental stages, including 1-day-old eggs, first-to fourth-instar larvae, prepupae, pupae, and adults, were collected for temporal expression analysis. For spatial expression analysis, specific tissues from fourth-instar larvae (epidermis, Malpighian tubules, fat body, foregut, midgut, and hindgut) were collected. The larvae were dissected on RNAhold®Reagent (TransGen Biotech, Beijing, China) under stereomicroscope (Olympus, Tokyo, Japan) to maintain tissue freshness. Each sample had three replicates, with 30–50 individuals per replicate.

2.5 RNA extraction and cDNA synthesis

Total RNA was extracted from whole bodies or specific tissue using the TransZol reagent (TransGen Biotech, Beijing, China). RNA quality and purity were assessed with a NanoDrop1000 spectrophotometer (Thermo Scientific, Waltham, MA, United States) and further confirmed by agarose gel electrophoresis. First-strand cDNA was synthesized using the TransScript Synthesis Supermix (TransGen Biotech) with 1 μg of total RNA.

2.6 Real-time quantitative PCR (qPCR)

qPCR was performed using a CFX-96 real-time PCR system (Bio-Rad, Hercules, CA, United States) with TransStart®Green qPCR Supermix (TransGen Biotech), following the manufacturer's protocol. PCR amplification was carried out with the following conditions: 95°C for 5 min, followed by 40 cycles of 95°C for 15 s and 60°C for 30 s. A melting curve analysis was performed from 55°C to 95°C to verify primer specificity. The gene expression level was calculated using the $2^{-\Delta\Delta CT}$ method (Livak and Schmittgen, 2001) and normalized to the reference genes *elongation factor 1-alpha* (*EF1α*) and *18S ribosomal RNA* (*18S*) (Yang et al., 2020). All the qPCR primers are presented in Supplementary Table S1.

2.7 RNA interference (RNAi) and bioassay

The cDNA fragments of *CYP6SZ3*, *CYP6AEL1*, and *green fluorescent protein* (*GFP*, as a negative control) were used to design double-stranded RNA (dsRNA) primers (Supplementary Table S1) through E-RNAi (https://www.dkfz.de/signaling/e-rnai3/). These dsRNAs were synthesized *in vitro* using the TranscriptAid T7 High Yield Transcription Kit (Thermo Scientific, Wilmington, DE, United States). Each fourth-instar larva was injected with 200 ng dsRNA (1 μg/μL) of *CYP6SZ3*, *CYP6AEL1*, or *GFP* using a Nanoliter 2010 injector (World Precision Instruments, Sarasota, FL, United States). At 48 h after injection, whole-body samples were collected to assess RNAi efficiency. In a parallel experiment, surviving larvae were collected at 48 h after dsRNA injection and further treated with ethyl formate and benzothiazole at LC$_{30}$ and LC$_{50}$ concentrations, and the mortality was recorded 24 h later. Each treatment was conducted in four replicates, with 30 larvae per replicate.

2.8 Homology modeling and molecular docking

Three-dimensional models of ethyl formate and benzothiazole were obtained from PubChem (https://pubchem.ncbi.nlm.nih.gov/). The protein sequences of CYP6SZ3 and CYP6AEL1 were modeled using Swiss-Model server (https://swissmodel.expasy.org/). Discovery Studio Client v21.1 (Accelrys Inc., San Diego,
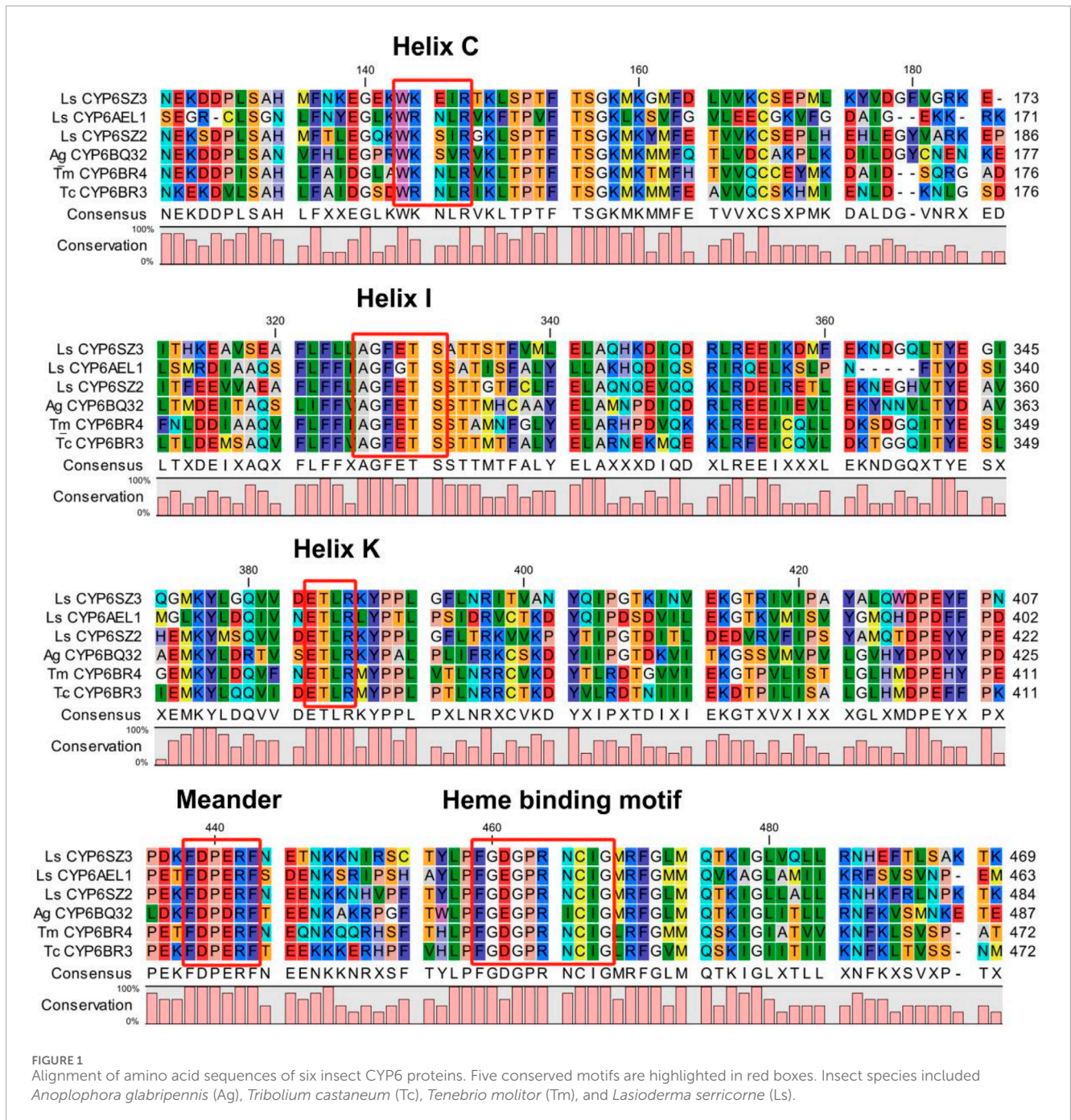
FIGURE 1
Alignment of amino acid sequences of six insect CYP6 proteins. Five conserved motifs are highlighted in red boxes. Insect species included *Anoplophora glabripennis* (Ag), *Tribolium castaneum* (Tc), *Tenebrio molitor* (Tm), and *Lasioderma serricorne* (Ls).

CA, United States) was used to identify potential fumigant ligand-binding pockets in the modeled CYP structures with default parameters. Binding free energies (ΔG_{bind}) between CYP proteins and fumigant ligands were calculated, and the outcomes were visualized using PyMOL (Delano Scientific, San Carlos, CA, United States).

2.9 Data analysis

Data are represented as the means ± standard error. Statistical differences were determined by one-way analysis of variance (ANOVA), followed by a least significant difference test or Student's t-test using SPSS 20.0 software.

3 Results

3.1 Toxicity of fumigants against *L. serricorne* larvae

The toxicity of two fumigants was evaluated on fourth-instar larvae using the sealed fumigation method with wide-mouth bottles. The LC_{30} values for ethyl formate and benzothiazole were

FIGURE 2
Phylogenetic analysis of CYP3 clan proteins in Coleopteran insects. The tree was constructed using the neighbor-joining method with 1,000 bootstrap replicates. The sequences of *L. serricorne* CYP6SZ3 and CYP6AEL1 are highlighted in red font. Insect species included *Anoplophora glabripennis* (Ag), *Tribolium castaneum* (Tc), *Tenebrio molitor* (Tm), and *Lasioderma serricorne* (Ls). GenBank accession numbers for all sequences are provided in the tree.

determined to be 19.344 and 396.751 $\mu L\ L^{-1}$, respectively. The LC_{50} values were 21.621 $\mu L\ L^{-1}$ for ethyl formate and 725.616 $\mu L\ L^{-1}$ for benzothiazole (Table 1).

3.2 Characterization of two CYP6 genes from *L. serricorne*

Two candidate *CYP6* genes were identified from *L. serricorne*, the full-length ORFs of *CYP6SZ1* and *CYP6AEL1* were verified by RT-PCR and named by David R. Nelson. The ORF sequences of *CYP6SZ1* and *CYP6AEL1* were 1,485 bp and 1,977 bp, encoding 494 and 656 amino acid residues, with predicted molecular weights of 56.69 kDa and 74.71 kDa and pI of 8.85 and 9.03, respectively. Sequence alignment analyses revealed that CYP6SZ1 and CYP6AEL1 contained five conserved motifs, including the helix C (WxxxR), helix I (AGxxTS), helix K (ExLR), meander (FxPxxF),

and heme binding (FxxGxxxCxG) (Figure 1). Phylogenetic analysis showed that both CYP6SZ3 and CYP6AEL1 belonged to the CYP3 clan from other insect species. The results showed that these CYPs clustered in five distinct families, and CYP6SZ3 and CYP6AEL1 belonged to the CYP6 family (Figure 2), with CYP6SZ3 closely related to CYP6SZ2 and CYP6SZ1 of *L. serricorne*, and CYP6AEL1 to CYP6BH3 of *Anoplophora glabripennis*.

3.3 Developmental and tissue-specific expression analysis

CYP6SZ3 and *CYP6AEL1* were expressed across all developmental stages of *L. serricorne*, from eggs to adults. The highest expression of *CYP6SZ3* was observed in the second-instar larvae, 13.6-fold higher than in the prepupa, which had the lowest expression level. *CYP6AEL1* showed the highest
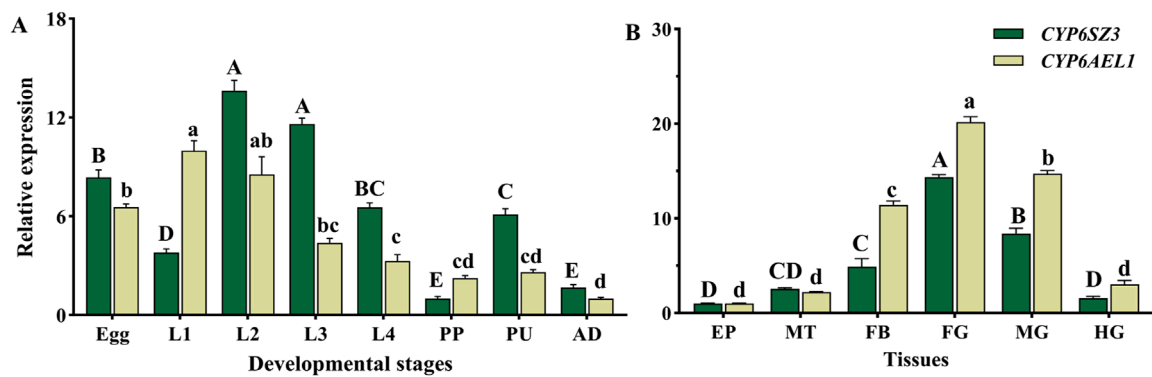
FIGURE 3
Relative expression levels of *CYP6SZ3* and *CYP6AEL1* across different developmental stages **(A)** and tissues **(B)** in *L. serricorne*. Stages: L1 (first-instar larvae), L2 (second-instar larvae), L3 (third-instar larvae), L4 (fourth-instar larvae), PP (prepupae), PU (pupae), and AD (adults). Tissues: EP (epidermis), MT (Malpighian tubules), FB (fat body), FG (foregut), MG (midgut), and HG (hindgut). Uppercase letters indicate significant differences in *CYP6SZ3* expression, and lowercase letters indicate significant differences in *CYP6AEL1* expression, based on one-way ANOVA followed by a least significant difference test ($P < 0.05$).
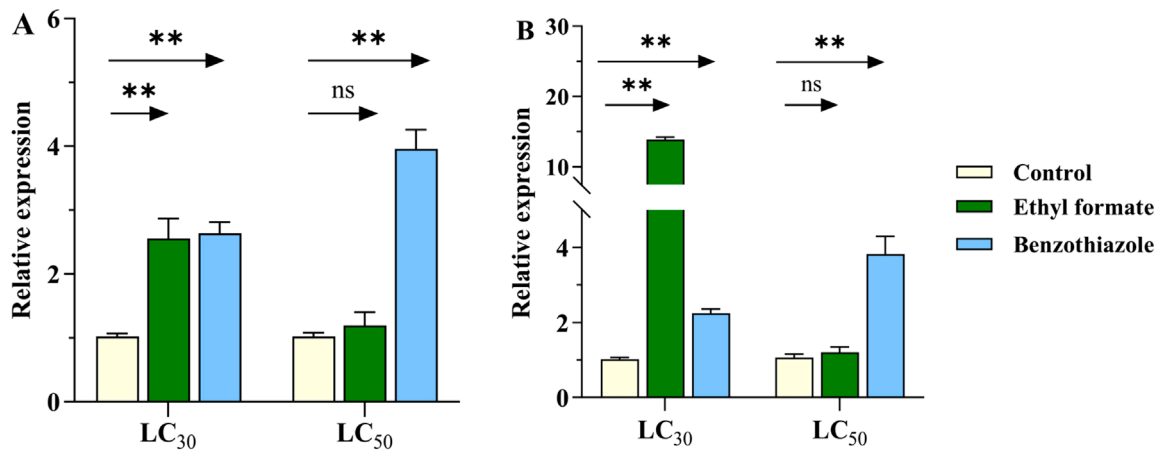

FIGURE 4
Effect of fumigant treatments on the expression levels of *CYP6SZ3* **(A)** and *CYP6AEL1* **(B)** in *L. serricorne*. Larvae exposed to normal air served as the negative control. Significant differences between the treatments and control at the same concentration were assessed using Student's *t*-test (**$P < 0.01$).

expression in the first-instar larvae, 9.9-fold higher than in adults (Figure 3A). *CYP6SZ3* and *CYP6AEL1* exhibited similar tissue-specific expression patterns, and both genes were mainly expressed in the foregut, midgut, and fat body, with the highest expression levels in the foregut,14.3-fold for *CYP6SZ3* and 20.2-fold for *CYP6AEL1* compared to the epidermis (Figure 3B).
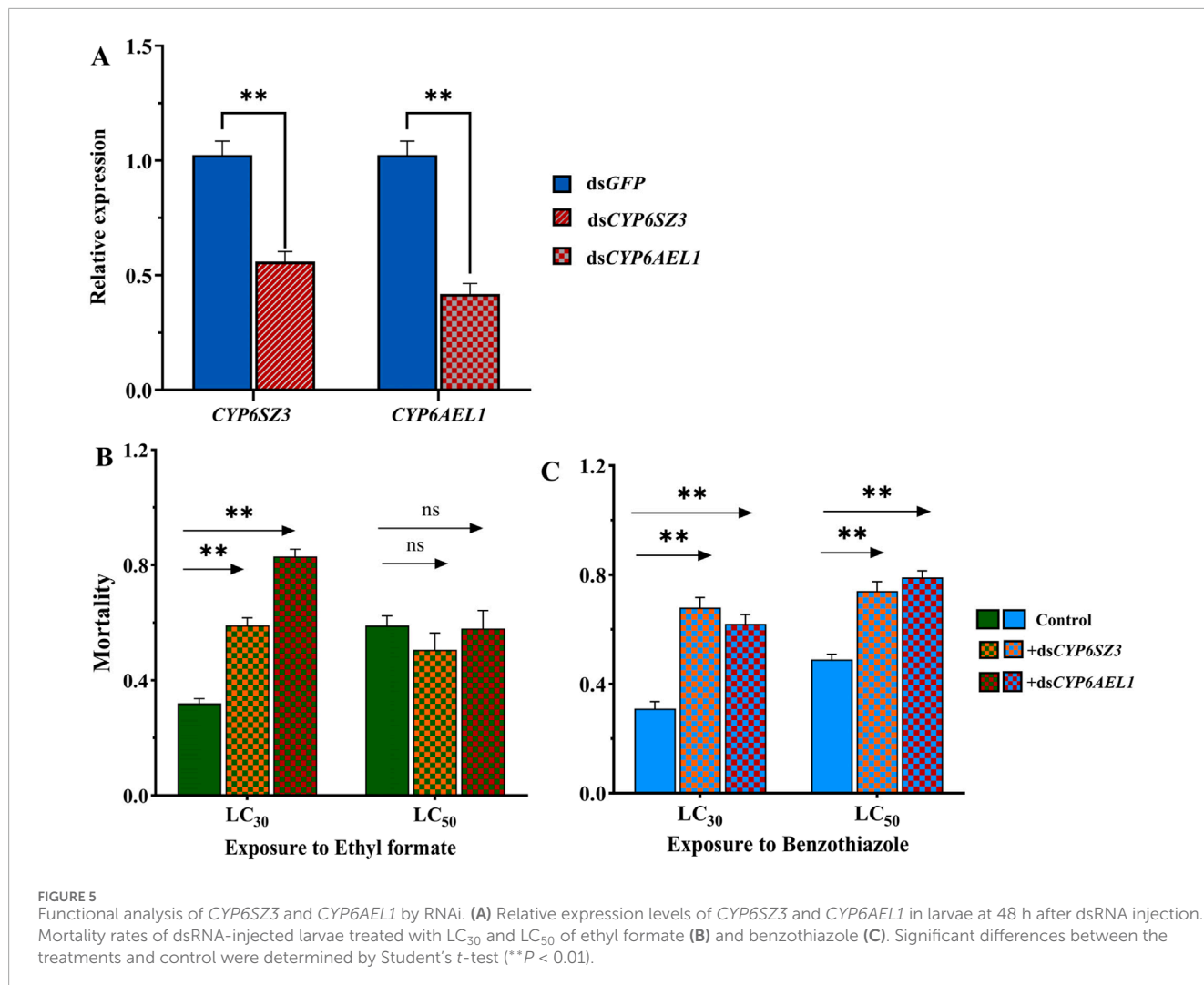
3.4 Expression patterns of two *CYP6* genes in response to fumigants

The expression of *CYP6SZ3* and *CYP6AEL1* increased significantly after treatment with LC_{30} of ethyl formate, showing 2.6- and 13.8-fold increases, respectively. However, no significant change was observed at LC_{50} concentrations. For benzothiazole exposure, expression of *CYP6SZ3* increased by 2.6- and 3.9-fold at

LC_{30} and LC_{50} concentrations, while *CYP6AEL1* showed 2.2- and 3.8-fold increases compared to the control (Figure 4).

3.5 Knockdown of *CYP6SZ3* and *CYP6AEL1* by RNAi

RNAi was performed in *L. serricorne* larvae to analyze the functions of *CYP6SZ3* and *CYP6AEL1* in fumigant detoxification. At 48 h after dsRNA injection, the expression levels of *CYP6SZ3* and *CYP6AEL1* were significantly decreased by 44.1% and 58.2% compared with the control, respectively (Figure 5A). The subsequent bioassay results showed that silencing both genes significantly increased susceptibility to LC_{30} of ethyl formate, with mortalities rising by 84.66% for *CYP6SZ3* and 159.37% for *CYP6AEL1*. No significant difference in mortality was observed after LC_{50} exposure

FIGURE 5
Functional analysis of *CYP6SZ3* and *CYP6AEL1* by RNAi. **(A)** Relative expression levels of *CYP6SZ3* and *CYP6AEL1* in larvae at 48 h after dsRNA injection. Mortality rates of dsRNA-injected larvae treated with LC_{30} and LC_{50} of ethyl formate **(B)** and benzothiazole **(C)**. Significant differences between the treatments and control were determined by Student's *t*-test (**$P < 0.01$).

to ethyl formate (Figure 5B). In contrast, after exposure to LC_{30} and LC_{50} of benzothiazole, mortality increased by 119.35% and 100% in the ds*CYP6SZ3* group and by 51.02% and 61.22% in the ds*CYP6AEL1* group (Figure 5C).

3.6 Homology modeling and fumigant docking

The three-dimensional structures of the CYP6SZ3 and CYP6AEL1 proteins were predicted using the Swiss-Model Server. Molecular docking was performed to investigate the binding interactions of these two CYP6 proteins with ethyl formate and benzothiazole. The docking models revealed strong interactions between both proteins and the compounds. For CYP6SZ3, the predicted binding site for ethyl formate included residues Lys72, Phe69, Asp68, Phe65, and Ile39, forming hydrogen bonds, carbon-hydrogen bonds, alkyl, and Pi-alkyl interactions with distances of 1.8, 3.0, 2.7, 2.6, and 5.3Å, respectively (Figure 6A). The binding site for benzothiazole involved residues Lys72, Phe65, and Ile39, with hydrogen bonds, Pi-sulfur, and Pi-alkyl interactions at distances of 1.9, 4.6, and 5.2Å (Figure 6B). For CYP6AEL1, the predicted

binding site for ethyl formate involved residues Val190, Val189, and Val141, engaging in alkyl and carbon-hydrogen bonds at distances of 4.7, 2.5, and 4.4Å (Figure 6C). The binding site for benzothiazole included Lys72, with Pi-cation and Pi-alkyl interactions at distances of 3.8 and 4.3Å (Figure 6D). The binding energies for the CYP6SZ3-ethyl formate, CYP6SZ3-benzothiazole, CYP6AEL1-ethyl formate, and CYP6AEL1-benzothiazole were −94.68, −26.89, −70.85, and −26.88 kcal/mol, respectively.

4 Discussion

In the present study, two *CYP6* genes, *CYP6SZ3* and *CYP6AEL1*, were identified which belong to separate branches of the CYP6 family. The deduced amino acid sequences of two CYP6s contain five conserved motifs: WxxxR, AGxE/DTT/S, ExLR, PxxFxPE/DRF, and FxxGxRxCxG/A (Liang et al., 2015; Xu et al., 2024; Li et al., 2024). Many members of CYP6 family are known to play roles in xenobiotic metabolism, aiding in detoxification (Katsavou et al., 2022), such as *CYP6M2* and *CYP6P3* in *Anopheles gambiae* (Djouaka et al., 2008), and *CYP6ER1* and *CYP6AY1* in *Nilaparvata lugens* (Zhang et al., 2016). Two *CYP6* genes are also typically expressed differentially
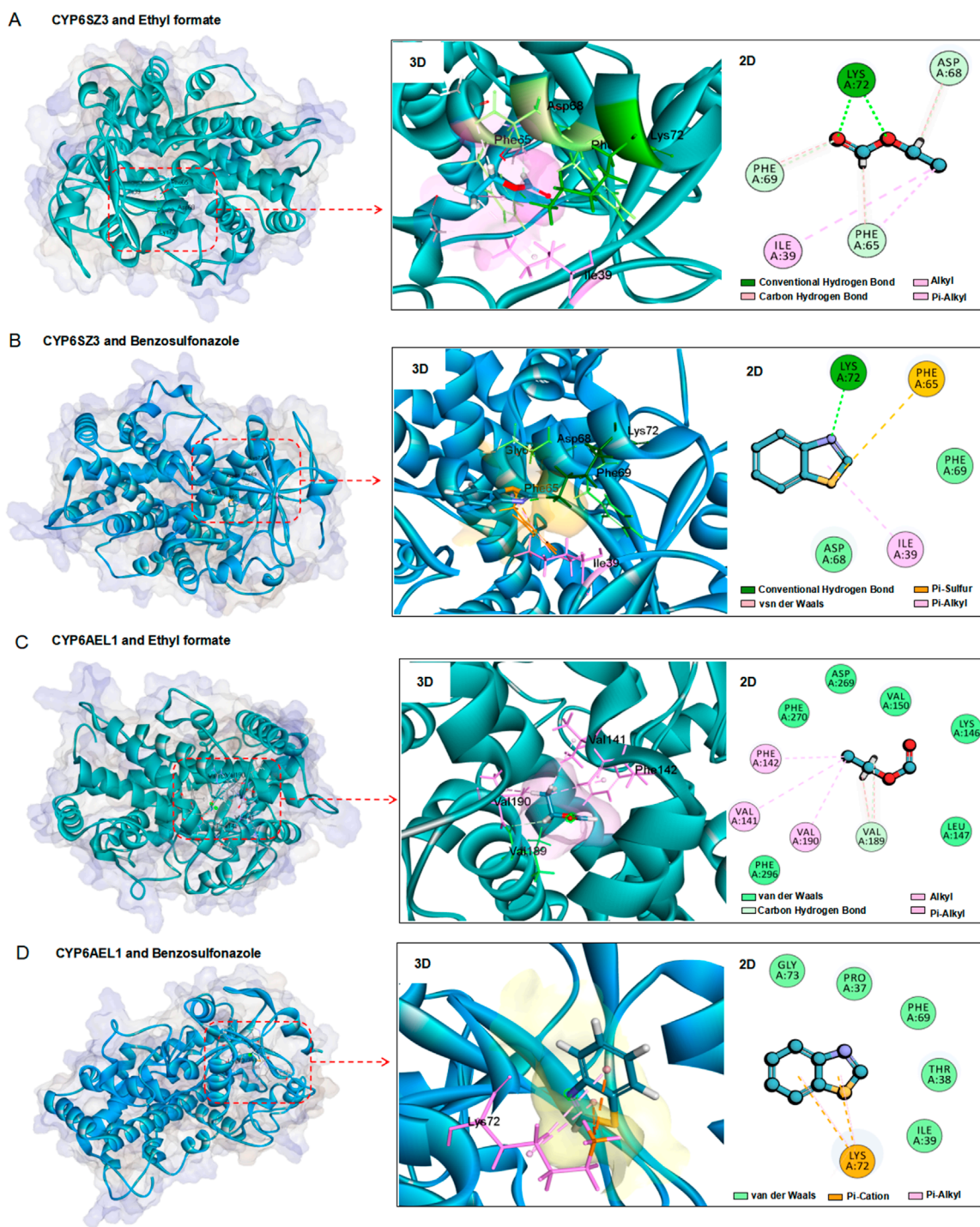
FIGURE 6
Homology modeling and fumigant docking. **(A, B)** Three-dimensional structures of CYP6SZ3 with two fumigants. **(C, D)** Three-dimensional structures of CYP6AEL1 with two fumigants. Amino acids within a distance of 6.0 Å from the docked ethyl formate or benzothiazole are enclosed in red boxes. Ethyl formate and benzothiazole are depicted as sticks, with oxygen in red, carbon in blue, sulfur in yellow, and nitrogen in purple.

across various developmental stages and tissues of *L. serricorne.* *CYP6SZ3* and *CYP6AEL1* showed higher expression levels in the larval stage, which is consistent with the expression patterns of other *CYP* genes like *CYP321A8*, *CYP321A9*, and *CYP321B1* in *Spodoptera frugiperda* (Zhang et al., 2020), and *CYP341B21*, *CYP341B37* in

Spodoptera litura (Li et al., 2024). On the other hand, lower expression levels were observed in the prepupal and adult stages, similar to *CYP353A1* in *T. castaneum* (Zhu et al., 2013). The tissue-specific expression patterns of these genes suggest a specialized role in insect metabolism. For example, CYP6E12 is highly expressed

in the fat body of *H. armigera* (Wang et al., 2018), while *CYP6BQ9* is predominantly expressed in the central nervous system and less so in the fat body of *T. castaneum* (Zhu et al., 2010). In this study, *CYP6SZ3* and *CYP6AEL1* exhibited high expression levels in the foregut, midgut, and fat body, tissues critical for detoxification in insects. The midgut and fat body play key roles in neutralizing allelochemicals (Skowronek et al., 2021; Zhu et al., 2011; Zeng et al., 2024), and the high expression levels in these tissues suggest that *CYP6SZ3* and *CYP6AEL1* are important for detoxifying insecticides.

Increased metabolic detoxification is often associated with the overexpression or induction of CYPs (Zhu et al., 2010; Wang et al., 2020). Therefore, this study focused on the role of the significantly induced CYP6 family in detoxifying fumigants. The results showed that the expression of *CYP6SZ3* and *CYP6AEL1* was significantly induced after exposure to LC_{30} doses of ethyl formate and benzothiazole, indicating their potential role in fumigant detoxification. However, no significant change was observed at the LC_{50} concentration of ethyl formate, possibly because higher doses might not allow enough time for the upregulation of protective CYPs before irreversible toxicity sets in. This trend is similar to what has been observed in *N. lugens*, where overexpression of *CYP6ER1* was limited under higher doses of imidacloprid (Bass et al., 2011). At higher doses, the toxic effects of ethyl formate on *L. serricorne* larvae may suppress detoxification functions or trigger apoptosis. Another possibility is that other detoxification genes, rather than *CYP6* genes, may play a dominant role when induced by high doses of ethyl formate, as seen with the co-involvement of *CYP6* and *CYP4* in imidacloprid metabolism in *N. lugens* (Zhang et al., 2016). Further investigation is needed to test these hypotheses.

Although *CYP6SZ3* and *CYP6AEL1* are potentially involved in the detoxification of ethyl formate and benzothiazole, their exact roles remain unclear. To explore their contribution to insecticide sensitivity, RNAi-based reverse genetics approaches were used (Li et al., 2024; Zhang Z. X. et al., 2023). After RNAi treatment, the expression of *CYP6SZ3* and *CYP6AEL1* was significantly reduced, resulting in increased mortality in *L. serricorne* when exposed to ethyl formate or benzothiazole. These results suggest that downregulation of these genes increases susceptibility to fumigants. Several CYP6 family genes from Coleopteran insects have been functionally analyzed for their roles in insecticide detoxification. For example, silencing of *CYP6BJa/b* and *CYP6BJ1v1* in *Leptinotarsa decemlineata* increases susceptibility to neonicotinoids (Kalsi and Palli, 2017). Similarly, dsRNA-mediated knockdown of *CYP6BQ9* in *T. castaneum* has been shown to enhance susceptibility to deltamethrin (Zhu et al., 2010), a finding further supported by *in vitro* detoxification studies. Suppressing *CYP6BQ11* expression has been found to increase susceptibility of *T. castaneum* to dichlorvos and carbofuran (Xiong et al., 2019). Based on these findings, it is likely that *CYP6SZ3* and *CYP6AEL1* contribute to enhanced tolerance against ethyl formate and benzothiazole. However, it is necessary to make clear whether *CYP6SZ3* and *CYP6AEL1* have the function of metabolizing ethyl formate and benzothiazole, the subsequent fumigant metabolism assays is needed.

Molecular modeling and docking analyses were performed to investigate the mechanism by which these two CYP6 proteins interact with fumigants. Molecular docking is a powerful tool for predicting interactions between insecticides and detoxification enzymes (Xiao and Lu, 2022; Tang et al., 2024). In this study, human

CYP3A4 and CYP3A5 were used as templates to build models for CYP6SZ3 and CYP6AEL1. The docking results indicated that both ethyl formate and benzothiazole bind strongly to CYP6SZ3 and CYP6AEL1. Several key residues, mostly hydrophobic amino acids such as Phe, Val, Leu, and Ile, appear to be involved in the binding (Zhu et al., 2010; Zhu et al., 2013). The binding free energies for CYP6SZ3 and CYP6AEL1 with the fumigants ranged from -26.88 to -94.68 kcal mol^{-1}, indicating strong binding affinities. These findings indicate that these genes might play essential roles in metabolizing the ethyl formate and benzothiazole, although further research involving heterologous expression and metabolic assays is required to confirm their metabolic capacity.

Data availability statement

The datasets presented in this study can be found in online repositories. The names of the repository/repositories and accession number(s) can be found in the article/Supplementary Material.

Author contributions

XL: Investigation, Writing–original draft. LM: Investigation, Methodology, Writing–original draft. WY: Writing–review and editing. KX: Conceptualization, Data curation, Funding acquisition, Project administration, Writing–review and editing.

Funding

Conflict of interest

The authors declare that the research was conducted in the absence of any commercial or financial relationships that could be construed as a potential conflict of interest.

Generative AI statement

The author(s) declare that no Generative AI was used in the creation of this manuscript.

Publisher's note

All claims expressed in this article are solely those of the authors and do not necessarily represent those of

their affiliated organizations, or those of the publisher, the editors and the reviewers. Any product that may be evaluated in this article, or claim that may be made by its manufacturer, is not guaranteed or endorsed by the publisher.

Supplementary material

The Supplementary Material for this article can be found online at: https://www.frontiersin.org/articles/10.3389/fphys.2024.1503953/full#supplementary-material

References

Aribou, Z. M., and Ng, W. T. (2022). Targeted medical examinations for workers exposed to fumigants. *J. Occup. Med. Toxicol.* 17, 20. doi:10.1186/s12995-022-00361-3

Austel, N., Schubert, J., Gadau, S., Jungnickel, H., Budnik, L. T., and Luch, A. (2017). Influence of fumigants on sunflower seeds: characteristics of fumigant desorption and changes in volatile profiles. *J. Hazard. Mater.* 337, 138–147. doi:10.1016/j.jhazmat.2017.04.070

Baliota, G. V., Edde, P. A., Kudithipudi, C., and Athanassiou, C. G. (2023). Effect of combining tobacco cultivars of different alkaloid contents on the development of *Lasioderma serricorne* (F.) (Coleoptera Anobiidae). *J. Stored Prod. Res.* 104, 102180. doi:10.1016/j.jspr.2023.102180

Bass, C., Carvalho, R. A., Oliphant, L., Puinean, A. M., Field, L. M., Nauen, R., et al. (2011). Overexpression of a cytochrome P450 monooxygenase, *CYP6ER1*, is associated with resistance to imidacloprid in the brown planthopper, *Nilaparvata lugens*. *Insect Mol. Biol.* 20, 763–773. doi:10.1111/j.1365-2583.2011.01105.x

Boyer, S., Lempérière, G., and Zhang, H. (2012). A review of control methods and resistance mechanisms in stored-product insects. *Bull. Entomol. Res.* 102, 213–229. doi:10.1017/S0007485311000654

Cui, K. D., He, L. M., Zhang, Z. Q., Zhang, L. Y., Mu, W., and Liu, F. (2020a). Effects of benzothiazole on survival for reduced reproduction and development in *Tribolium castaneum* Herbst (Coleoptera: tenebrionidae). *Pest Manag. Sci.* 76, 3088–3095. doi:10.1002/ps.5860

Cui, K. D., He, L. M., Zhang, Z. Q., Zhang, T., Mu, W., and Liu, F. (2020b). Evaluation of the efficacy of benzothiazole against the red flour beetle, *Tribolium castaneum* (Herbst). *Pest Manag. Sci.* 76, 2726–2735. doi:10.1002/ps.5819

Damcevski, K. A., Dojchinov, G., Woodman, J. D., and Haritos, V. S. (2010). Efficacy of vaporised ethyl formate/carbon dioxide formulation against stored-grain insects: effect of fumigant concentration, exposure time and two grain temperatures. *Pest Manag. Sci.* 66, 432–438. doi:10.1002/ps.1895

Dermauw, W., Van Leeuwen, T., and Feyereisen, R. (2020). Diversity and evolution of the P450 family in arthropods. *Insect biochem. Mol. Biol.* 127, 103490. doi:10.1016/j.ibmb.2020.103490

Djouaka, R. F., Bakare, A. A., Coulibaly, O. N., Akogbeto, M. C., Ranson, H., Hemingway, J., et al. (2008). Expression of the cytochrome P450s, *CYP6P3* and *CYP6M2* are significantly elevated in multiple pyrethroid resistant populations of *Anopheles gambiae s.s.* from Southern Benin and Nigeria. *BMC Genomics* 9, 538. doi:10.1186/1471-2164-9-538

Edde, P. A. (2019). Biology, ecology, and control of *Lasioderma serricorne* (F.) (Coleoptera: Anobiidae): a review. *J. Econ. Entomol.* 112, 1011–1031. doi:10.1093/jee/toy428

Feyereisen, R., and Gilbert, L. I. (2012). "Insect CYP genes and P450 enzymes," in *Insect molecular biology and biochemistry* (San Diego: Academic Press), 236–316.

Haritos, V. S., and Dojchinov, G. (2003). Cytochrome c oxidase inhibition in the rice weevil *Sitophilus oryzae* (L.) by formate, the toxic metabolite of volatile alkyl formates. *Comp. Biochem. Physiol. C Toxicol. Pharmacol.* 136, 135–143. doi:10.1016/s1532-0456(03)00173-x

Kalsi, M., and Palli, S. R. (2017). Transcription factor cap n collar C regulates multiple cytochrome P450 genes conferring adaptation to potato plant allelochemicals and resistance to imidacloprid in *Leptinotarsa decemlineata* (Say). *Insect biochem. Mol. Biol.* 83, 1–12. doi:10.1016/j.ibmb.2017.02.002

Katsavou, E., Riga, M., Ioannidis, P., King, R., Zimmer, C. T., and Vontas, J. (2022). Functionally characterized arthropod pest and pollinator cytochrome P450s associated with xenobiotic metabolism. *Pestic. Biochem. Physiol.* 181, 105005. doi:10.1016/j.pestbp.2021.105005

Kim, B. S., Shin, E. M., Park, Y. J., and Yang, J. O. (2020). Susceptibility of the cigarette beetle *Lasioderma serricorne* (Fabricius) to phosphine, ethyl formate and their combination, and the sorption and desorption of fumigants on cured tobacco leaves. *Insects* 11, 599. doi:10.3390/insects11090599

Kim, K. N., Kim, D. B., Kwon, S. H., Roh, G. H., Lee, S. M., Lee, B. H., et al. (2023). A novel ethyl formate fumigation strategy for managing yellow tea thrips (*Scirtothrips dorsalis*) in greenhouse cultivated mangoes and post-harvest fruits. *Insects* 14, 568. doi:10.3390/insects14060568

Kumar, S., Stecher, G., and Tamura, K. (2016). MEGA7: molecular evolutionary genetics analysis version 7.0 for bigger datasets. *Mol. Biol. Evol.* 33, 1870–1874. doi:10.1093/molbev/msw054

Li, P. R., Shi, Y., Ju, D., Liu, Y. X., Wang, W., He, Y. S., et al. (2023). Metabolic functional redundancy of the *CYP9A* subfamily members leads to P450-mediated *lambda*-cyhalothrin resistance in *Cydia pomonella*. *Pest Manage. Sci.* 79, 1452–1466. doi:10.1002/ps.7317

Li, W. L., Yang, W., Shi, Y., Yang, X. Y., Liu, S. Q., Liao, X. L., et al. (2024). Comprehensive analysis of the overexpressed cytochrome P450-based insecticide resistance mechanism in *Spodoptera litura*. *J. Hazard. Mater.* 461, 132605. doi:10.1016/j.jhazmat.2023.132605

Li, X. C., Schuler, M. A., and Berenbaum, M. R. (2007). Molecular mechanisms of metabolic resistance to synthetic and natural xenobiotics. *Annu. Rev. Entomol.* 52, 231–253. doi:10.1146/annurev.ento.51.110104.151104

Liang, X., Xiao, D., He, Y. P., Yao, J. X., Zhu, G. N., and Zhu, K. Y. (2015). Insecticide-mediated up-regulation of cytochrome P450 genes in the red flour beetle (*Tribolium castaneum*). *Int. J. Mol. Sci.* 16, 2078–2098. doi:10.3390/ijms16012078

Livak, K. J., and Schmittgen, T. D. (2001). Analysis of relative gene expression data using real-time quantitative PCR and the $2^{-\Delta\Delta CT}$ method. *Methods* 25, 402–408. doi:10.1006/meth.2001.1262

Lu, K., Song, Y., and Zeng, R. (2021). The role of cytochrome P450-mediated detoxification in insect adaptation to xenobiotics. *Curr. Opin. Insect Sci.* 43, 103–107. doi:10.1016/j.cois.2020.11.004

Maille, J. M., Edde, P. A., and Phillips, T. W. (2023). Efficacy of propylene oxide and ethyl formate as fumigants to control *Lasioderma serricorne* (F.) (Coleoptera: ptinidae). *J. Stored Prod. Res.* 100, 102047. doi:10.1016/j.jspr.2022.102047

Mithlesh, P. P. K., Kant, R., Shukla, S. K., and Ojha, K. G. (2010). Rapid synthesis and biological evaluation of 1,4-dihydropyridine derivatives containing a benzothiazolyl moiety. *Cent. Eur. J. Chem.* 8, 163–173. doi:10.2478/s11532-009-0114-z

Nayak, M. K., Daglish, G. J., Phillips, T. W., and Ebert, P. R. (2020). Resistance to the fumigant phosphine and its management in insect pests of stored products: a global perspective. *Annu. Rev. Entomol.* 65, 333–350. doi:10.1146/annurev-ento-011019-025047

Qin, P. H., Zheng, H. Y., Tao, Y. L., Zhang, Y. J., and Chu, D. (2023). Genome-wide identification and expression analysis of the cytochrome P450 gene family in *Bemisia tabaci* MED and their roles in the insecticide resistance. *Int. J. Mol. Sci.* 24, 5899. doi:10.3390/ijms24065899

Ren, Y. L., and Mahon, D. (2006). Fumigation trials on the application of ethyl formate to wheat, split faba beans and sorghum in small metal bins. *J. Stored Prod. Res.* 42, 277–289. doi:10.1016/j.jspr.2005.04.002

Sağlam, Ö., Edde, P. A., and Phillips, T. W. (2015). Resistance of *Lasioderma serricorne* (Coleoptera: Anobiidae) to fumigation with phosphine. *J. Econ. Entomol.* 108, 2489–2495. doi:10.1093/jee/tov193

Schuler, M. A. (2011). P450s in plant-insect interactions. *Biochim. Biophys. Acta.* 1814, 36–45. doi:10.1016/j.bbapap.2010.09.012

Skowronek, P., Wójcik, Ł., and Strachecka, A. (2021). Fat body–multifunctional insect tissue. *Insects* 12, 547. doi:10.3390/insects12060547

Smit, R., Jooste, M. M., Addison, M. F., and Johnson, S. A. (2020). Ethyl formate fumigation: its effect on stone and pome fruit quality, and grain chinch bug (*Macchiademus diplopterus*) mortality. *Sci. Hortic.* 261, 108845. doi:10.1016/j.scienta.2019.108845

Tang, J., Zhang, Q. H., Qu, C., Su, Q., Luo, C., and Wang, R. (2024). Knockdown of one cytochrome P450 gene *CYP6DW4* increases the susceptibility of *Bemisia tabaci* to dimpropyridaz, a novel pyridazine pyrazolecarboxamide insecticide. *Pestic. Biochem. Physiol.* 201, 105888. doi:10.1016/j.pestbp.2024.105888

Tsakireli, D., Riga, M., Kounadi, S., Douris, V., and Vontas, J. (2019). Functional characterization of *CYP6A51*, a cytochrome P450 associated with pyrethroid resistance in the Mediterranean fruit fly *Ceratitis capitata*. *Pestic. Biochem. Physiol.* 157, 196–203. doi:10.1016/j.pestbp.2019.03.022

Wang, H. D., Shi, Y., Wang, L., Liu, S., Wu, S. W., Yang, Y. H., et al. (2018). *CYP6AE* gene cluster knockout in *Helicoverpa armigera* reveals role in detoxification of phytochemicals and insecticides. *Nat. Commun.* 9, 4820. doi:10.1038/s41467-018-07226-6

Wang, K. X., Liu, M. W., Wang, Y. Z., Song, W., and Tang, P. A. (2020). Identification and functional analysis of cytochrome P450 *CYP346* family genes associated with

phosphine resistance in *Tribolium castaneum*. *Pestic. Biochem. Physiol.* 168, 104622. doi:10.1016/j.pestbp.2020.104622

Wang, R., Zhu, Y., Deng, L., Zhang, H., Wang, Q., Yin, M., et al. (2017). Imidacloprid is hydroxylated by *Laodelphax striatellus* CYP6AY3v2. *Insect. Mol. Biol.* 26, 543–551. doi:10.1111/imb.12317

Xiao, T. X., and Lu, K. (2022). Functional characterization of *CYP6AE* subfamily P450s associated with pyrethroid detoxification in *Spodoptera litura*. *Int. J. Biol. Macromol.* 219, 452–462. doi:10.1016/j.ijbiomac.2022.08.014

Xiong, W. F., Gao, S. S., Mao, J. J., Wei, L. T., Xie, J., Liu, J. J., et al. (2019). *CYP4BN6* and *CYP6BQ11* mediate insecticide susceptibility and their expression is regulated by Latrophilin in *Tribolium castaneum*. *Pest Manag. Sci.* 75, 2744–2755. doi:10.1002/ps.5384

Xu, L., Zhao, J., Xu, D. J., Xu, G. C., Peng, Y. C., and Zhang, Y. N. (2024). New insights into chlorantraniliprole metabolic resistance mechanisms mediated by the striped rice borer cytochrome P450 monooxygenases: a case study of metabolic differences. *Sci. Total Environ.* 912, 169229. doi:10.1016/j.scitotenv.2023.169229

Yan, Y., Xu, K. K., Yang, H., Hu, D. M., and Yang, W. J. (2020). Expression of glutathione S-transferase gene *LsGSTe1* and its relationship with ethyl formate tolerance in the cigarette beetle, *Lasioderma serricorne* (Coleoptera: Anobiidae). *Acta Entomol. Sin.* 63, 1–10. doi:10.16380/j.kcxb.2020.01.001

Yang, W. J., Xu, K. K., Cao, Y., Meng, Y. L., Liu, Y., and Li, C. (2019). Identification and expression analysis of four small heat shock protein genes in cigarette beetle, *Lasioderma serricorne* (Fabricius). *Insects* 10, 139. doi:10.3390/insects10050139

Yang, W. J., Xu, K. K., Yan, Y., Li, C., and Jin, D. C. (2020). Role of *Chitin deacetylase 1* in the molting and metamorphosis of the cigarette beetle *Lasioderma serricorne*. *Int. J. Mol. Sci.* 21, 2449. doi:10.3390/ijms21072449

Yang, Y. H., Yue, L. N., Chen, S., and Wu, Y. D. (2008). Functional expression of *Helicoverpa armigera* CYP9A12 and CYP9A14 in *Saccharomyces cerevisiae*. *Pestic. Biochem. Physiol.* 92, 101–105. doi:10.1016/j.pestbp.2008.07.001

Zaitoon, A., Jabeen, A., Ahenkorah, C., Scott-Dupree, C., and Lim, L. T. (2021). In-package fumigation of blueberries using ethyl formate: effects on spotted-wing drosophila (*Drosophila suzukii* Matsumura) mortality and fruit quality. *Food Packag. Shelf Life* 30, 100717. doi:10.1016/j.fpsl.2021.100717

Zeng, T., Teng, F., Wei, H., Lu, Y., Xu, Y., and Qi, Y. (2024). AANAT1 regulates insect midgut detoxification through the ROS/CncC pathway. *Commun. Biol.* 7, 808. doi:10.1038/s42003-024-06505-x

Zhang, B. Z., Su, X., Zhen, C. A., Lu, L. Y., Li, Y. S., Ge, X., et al. (2020). Silencing of cytochrome P450 in *Spodoptera frugiperda* (Lepidoptera: noctuidae) by RNA interference enhances susceptibility to chlorantraniliprole. *J. Insect Sci.* 20, 12. doi:10.1093/jisesa/ieaa047

Zhang, C., Ma, Z. Q., Zhang, X., and Wu, H. (2017). Transcriptomic alterations in *Sitophilus zeamais* in response to allyl isothiocyanate fumigation. *Pestic. Biochem. Physiol.* 137, 62–70. doi:10.1016/j.pestbp.2016.10.001

Zhang, L. J., Wei, Y. J., Wei, L. Y., Liu, X. N., and Liu, N. (2023a). Effects of transgenic cotton lines expressing ds*AgCYP6CY3–P1* on the growth and detoxification ability of *Aphis gossypii* glover. *Pest Manag. Sci.* 79, 481–488. doi:10.1002/ps.7220

Zhang, Y. C., Gao, S. S., Xue, S., An, S. H., and Zhang, K. P. (2021). Disruption of the cytochrome P450 *CYP6BQ7* gene reduces tolerance to plant toxicants in the red flour beetle. *Tribolium Castaneum. Int. J. Biol. Macromol.* 172, 263–269. doi:10.1016/j.ijbiomac.2021.01.054

Zhang, Y. X., Yang, Y. X., Sun, H. H., and Liu, Z. W. (2016). Metabolic imidacloprid resistance in the brown planthopper, *Nilaparvata lugens*, relies on multiple P450 enzymes. *Insect biochem. Mol. Biol.* 79, 50–56. doi:10.1016/j.ibmb.2016.10.009

Zhang, Z. X., Wang, D., Shan, Y. P., Chen, J. X., Hu, H. Y., Song, X. P., et al. (2023b). Knockdown of *CYP9A9* increases the susceptibility to lufenuron, methoxyfenozide and a mix of both in *Spodoptera exigua*. *Insect Mol. Biol.* 32, 263–276. doi:10.1111/imb.12829

Zhao, Y. H., Xu, C. M., Wang, Q. H., Wei, Y., Liu, F., Xu, S. Y., et al. (2016a). Effects of the microbial secondary metabolite benzothiazole on the nutritional physiology and enzyme activities of *Bradysia odoriphaga* (Diptera: sciaridae). *Pestic. Biochem. Physiol.* 129, 49–55. doi:10.1016/j.pestbp.2015.10.017

Zhao, Y. H., Zhang, P., Zhai, Y. B., Chen, C. Y., Wang, Q. H., Han, J. K., et al. (2016b). Sublethal concentration of benzothiazole adversely affect development, reproduction and longevity of *Bradysia odoriphaga* (Diptera: sciaridae). *Phytoparasitica* 44, 115–124. doi:10.1007/s12600-016-0506-5

Zhu, F., Moural, T. W., Shah, K., and Palli, S. R. (2013). Integrated analysis of cytochrome P450 gene superfamily in the red flour beetle, *Tribolium castaneum*. *BMC Genomics* 14, 174. doi:10.1186/1471-2164-14-174

Zhu, F., Parthasarathy, R., Bai, H., Woithe, K., Kaussmann, M., Nauen, R., et al. (2010). A brain-specific cytochrome P450 responsible for the majority of deltamethrin resistance in the QTC279 strain of *Tribolium castaneum*. *Proc. Natl. Acad. Sci. U. S. A.* 107, 8557–8562. doi:10.1073/pnas.1000059107

Zhu, Y. C., Guo, Z. B., Chen, M. S., Zhu, K. Y., Liu, X. F., and Scheffler, B. (2011). Major putative pesticide receptors, detoxification enzymes, and transcriptional profile of the midgut of the tobacco budworm, *Heliothis virescens* (Lepidoptera: noctuidae). *J. Invertebr. Pathol.* 106, 296–307. doi:10.1016/j.jip.2010.10.007

Zimmer, C. T., Bass, C., Williamson, M. S., Kaussmann, M., Wölfel, K., Gutbrod, O., et al. (2014). Molecular and functional characterization of *CYP6BQ23*, a cytochrome P450 conferring resistance to pyrethroids in European populations of pollen beetle, *Meligethes aeneus*. *Insect biochem. Mol. Biol.* 45, 18–29. doi:10.1016/j.ibmb.2013.11.008